Redox Biology 51 (2022) 102270

Contents lists available at ScienceDirect

Redox Biology

journal homepage: www.elsevier.com/locate/redox

MPTAC links alkylation damage signaling to sterol biosynthesis

Tamaki Suganuma *, Jerry L. Workman

Stowers Institute for Medical Research, 1000 E. 50th Street, Kansas City, MO, 64110, USA

ARTICLE INFO

Keywords:
MPTAC
ATAC
MSH6
Alkylation damage
Mevalonate pathway
Sterol biosynthesis
Fragile X-associated disorders

ABSTRACT

Overproduction of reactive oxygen species (ROS) drives inflammation and mutagenesis. However, the role of the DNA damage response in immune responses remains largely unknown. Here we found that stabilization of the mismatch repair (MMR) protein MSH6 in response to alkylation damage requires interactions with the molybdopterin synthase associating complex (MPTAC) and Ada2a-containing histone acetyltransferase complex (ATAC). Furthermore, MSH6 promotes sterol biosynthesis via the mevalonate pathway in a MPTAC- and ATAC-dependent manner. MPTAC reduces the source of alkylating agents (ROS). Therefore, the association between MMR proteins, MPTAC, and ATAC promotes anti-inflammation response and reduces alkylating agents. The inflammatory responses measured by xanthine oxidase activity are elevated in Lymphoblastoid Cell Lines (LCLs) from some Fragile X-associated disorders (FXD) patients, suggesting that alkylating agents are increased in these FXD patients. However, MPTAC is disrupted in LCLs from some FXD patients. In LCLs from other FXD patients, interaction between MSH6 and ATAC was lost, destabilizing MSH6. Thus, impairment of MPTAC and ATAC may cause alkylation damage resistance in some FXD patients.

1. Introduction

Numerous viruses reduce respiration in host tissue to obtain energy [1]. This reprogramming induces hypoxic responses, most of which are mediated by hypoxia-inducible factor 1 subunit alpha (HIF1A) [1]. Hypoxia-induced proinflammatory cytokines promote expression of xanthine dehydrogenase (XDH), whose enzymatic activity requires molybdenum cofactor (Moco) and Moco biosynthetic enzymes including molybdopterin (MPT) synthase [2,3]. Post-translational conversion of XDH to xanthine oxidase (XO) is a conversion from a source of reducing equivalents to a source of ROS [2]. In hypoxic conditions, XO generates hydrogen peroxide (H_2O_2), which promotes the activity of human immunodeficiency virus [4].

In response to viral infection, activation of dsRNA-dependent protein kinase R (PKR) inhibits initiation of mRNA translation to prevent viral protein synthesis [5]. In hypoxia, PKR suppresses HIF1A transcription [6]. The association of MPT synthase with ATAC suppresses PKR autophosphorylation and activation and promotes iron-responsive mRNA translation [5].

MPT synthase (a heterotetramer of MOCS2A and MOCS2B dimers) forms the MPT synthase associating complex (MPTAC) by associating with MOCS3, DBN1, CLNS1A, SNRPD2, SNRPB/B′, and HSD17B10 [7]. MOCS3 reactivates MOCS2A for the next cycle of cPMP conversion during Moco biosynthesis [8]. MPTAC is required for sulfur amino acid catabolism that promotes fatty acid β-oxidation and prevents the generation of pathological amyloid-β (Aβ) deposition found in Alzheimer's disease [7]. MPTAC also suppresses ROS generation and is required for maintaining cellular S-adenosylmethionine (SAMe) levels [7]. The MPTAC subunit MOCS2 is required for formation of MPTAC and is crucial for XDH activity [2,3,7].

A connection between the pathogenesis of Alzheimer's disease (AD) and Fragile X syndrome (FXS) has been suggested since increased Aβ formation has been observed in a fragile X mental retardation 1 gene (*Fmr1*)-knockout FXS mouse model [9]. Fragile X-associated disorders (FXD) including FXS, fragile X-associated tremor/ataxia syndrome (FXTAS), and fragile X-associated primary ovarian insufficiency (FXPOI) are characterized by X-linked inherited intellectual disability or cognitive decline [10]. FXD are caused by CGG repeat expansion in the 5′ untranslated region of the *FMR1* [11]. FXTAS and FXPOI carry 55–200 CGG repeats (fragile X "premutation") [11], whereas FXS carries >200 CGG repeats ("full mutation") [10]. Females who are heterozygotes for the premutation, particularly in those with FXTAS, have a higher rate of immune-mediated disorders (IMDs), rheumatoid arthritis, and thyroid disorders than female noncarriers [12]. However, some FXTAS individuals carry 45–54 CGG repeats and associate with cognitive decline [11,13]. Other factors in addition to CGG repeats expansion are

* Corresponding author.
E-mail addresses: tas@stowers.org (T. Suganuma), jlw@stowers.org (J.L. Workman).

https://doi.org/10.1016/j.redox.2022.102270
Received 3 December 2021; Received in revised form 1 February 2022; Accepted 14 February 2022
Available online 16 February 2022

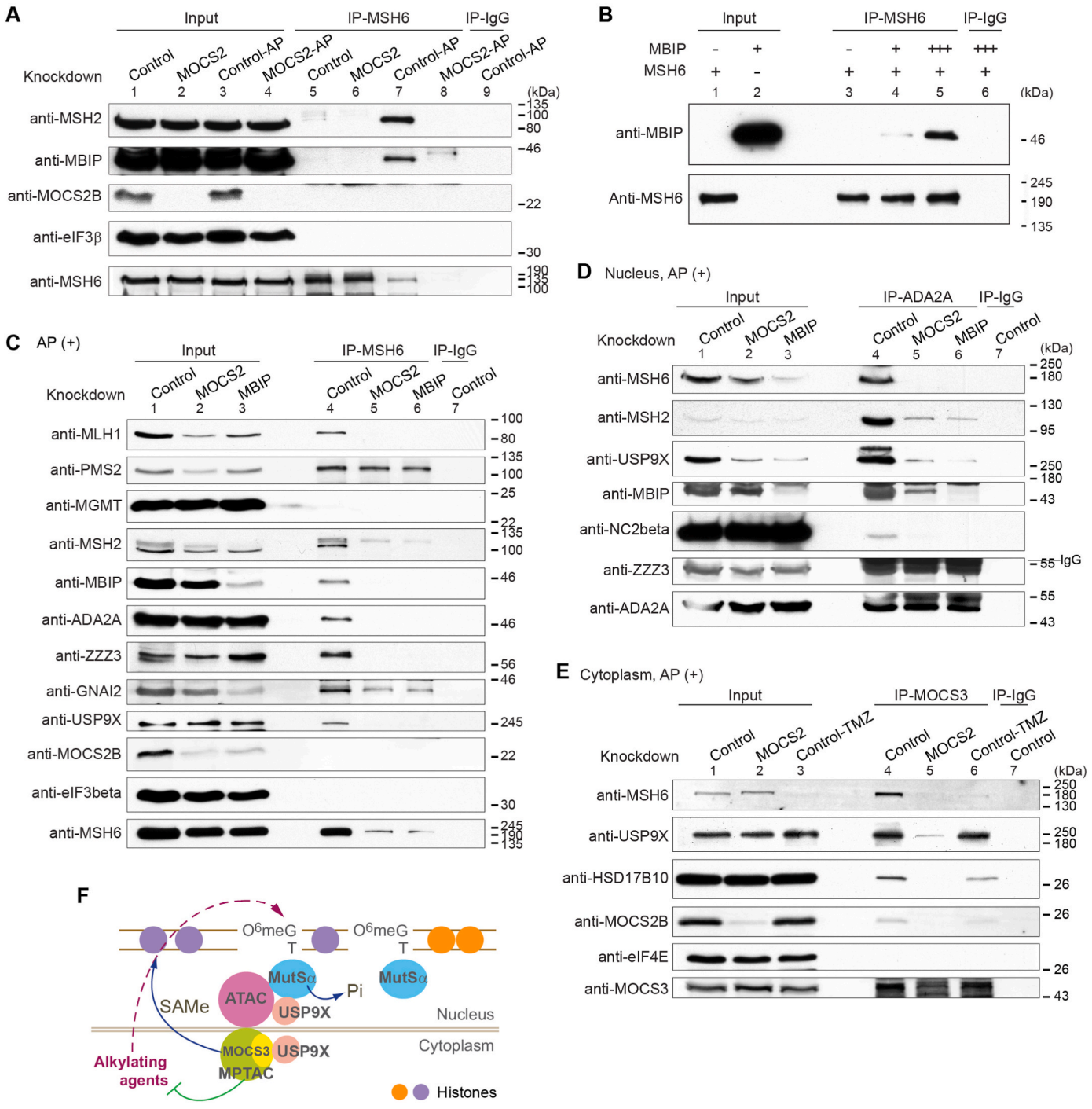

Fig. 1. Associations of DNA mismatch repair proteins require MOCS2 and MBIP.
(A) MSH6 immunoprecipitation (IP) in nuclear extracts from MOCS2-knockdown and control HEK293 cells with or without alkaline phosphatase (AP) treatment were examined by Western blot. IgG immunoprecipitates were used as a control; eIF3β was the loading control. **(B)** Purified recombinant MBIP from Sf21 cells interacts directly with recombinant MSH6. **(C)** MSH6 IP in nuclear extracts from indicated knockdown cells treated with AP. eIF3β was the loading control. **(D)** ADA2A IP in AP-treated nuclear extracts were examined by Western blot. **(E)** MOCS3 IP in AP-treated cytoplasmic extracts were examined by Western blot. Control HEK293 cells treated with 100 mM TMZ for 48 h were also examined. eIF4E was the loading control. **(F)** Summery model describes the connections of MMR with MPTAC and ATAC.

suggested to influence the variety of medical problems.

Here we investigated whether MPTAC and ATAC participate in cellular responses to alkylation DNA damage, and whether alkylation DNA damage signaling is disrupted in FXD. We found that XDH activity is increased in LCLs from FXD patients. Therefore, we hypothesize that MPTAC and ATAC may be involved in the pathogenesis of FXD.

2. Material and methods

2.1. Examination of knockdown HEK293 cells

Methods of cell extraction and CRISPR knockdown are described in supplementary material and methods.

2.2. Culture of human lymphoblastoid cell lines

LCLs from B-lymphocytes from FXD patients and healthy doners (listed in Supplementary Table 1) were provided by the Coriell Institute for Medical Research and were cultured in RPMI 1640 medium containing 2 mM L-glutamine and 15% Fetal Bovine Serum at 37 °C under 5% CO_2. Some of the cells were treated with 100 mM TMZ for 48 h at 37 °C under 5% CO_2 before harvesting. Information of the cell lines are provided on the Coriell Institute website: https://www.coriell.org/0/Sections/BrowseCatalog/DiseaseDetail.aspx?PgId=403&omim=MEN30955&coll=

2.3. Xanthine oxidase fluorometric assay

Cytoplasmic extracts were analyzed using a Xanthine Oxidase Fluorometric Assay Kit (Cayman, 10010895). Samples were diluted at a 1:3 ratio using sample buffer (10 mM 4-(2-Hydroxyethyl)-1-piperazine ethanesulfonic acid pH 7.5, 10 mM Potassium Chloride, 1.5 mM Magnesium chloride, and one Roche Complete EDTA-free Protease Inhibitor tablet per 15 mL buffer). Both initial and subsequent dilutions of the standard were done per protocol using sample buffer described above. In addition, the assay was miniaturized to 384 well format with a final well volume of 25 μL by reducing each component of the protocol by a factor of 4. The assay measured the production of the fluorescent compound resorufin (excitation 520–550 nm, emission 585–595 nm), produced by the reaction of H_2O_2 with 10-acetyl-3,7-dihydroxyphenoxiazine (ADHP) in a 1:1 stoichiometry in the presence of horseradish peroxidase. Absorbance was measured at 60, 75, and 90 min after XO substrate was added to the sample mixtures. The average background (sample buffer only, n = 3) was subtracted from all sample and standard curve values. The standard curve was plotted as a linear regression and the interpolation of the sample's values determined the XO concentration (μU/mL). The amount of XO for each sample was normalized to protein concentration and was plotted as mean ± SD. Each sample contained three technical replicates and the experiment assayed two biological replicates of each sample.

3. Results and discussion

3.1. DNA mismatch repair following DNA alkylation requires MPTAC and ATAC

We previously found that MPTAC suppresses the generation of ROS, which is the source of alkylating agents. Alkylating agents are byproducts of oxidative damage [14]. SAMe is methyl donor in reactions in which a single methyl group is transferred to a DNA base, DNA alkylating and nitrosating agents modify N^7-guanine (N^7G) and O^6-guanine (O^6G) to N^7-methylguanine (N^7meG) and O^6-methylguanine (O^6meG), respectively [15]. MOCS2 dependent SAMe is crucial for methylation of N^7G in mRNA [16]. In mismatch repair (MMR), mutS homologs 2 and 6 (MSH2 and MSH6) bind O^6meG:C [17] by forming the heterodimer complex MutSα. Phosphorylation of MSH6 increases its binding to G-T mismatches, promoting mismatch repair [18]. However, unphosphorylated MSH6 has a higher affinity for O^6meG, leading to MutSα binding O^6meG-T rather than G-T mismatches, and inducing DNA damage signaling by recruiting MutLα and DNA damage response proteins [15,17]. Cells deficient in MMR proteins such as MSH6 do not attempt to process O^6meG:C and O^6meG:T mismatches, therefore these cells are DNA damage-tolerant [18]. MSH6-deficient cells exhibit resistance to alkylating reagents [19]. Hence, we investigated whether MPTAC affects MMR proteins in response to O^6meG.

We first examined MutSα formation by performing MSH6 immunoprecipitation in nuclear extracts. We stored a part of each extract at −80 °C to be used as "input" samples for western blots. We incubated the remaining extracts with MSH6 antibody or IgG at 4 °C for 8 h. The interaction of MSH2 with MSH6 was significantly greater in cells treated with alkaline phosphatase (AP) for 30 min than in untreated cells (Fig. 1A, lanes 5 and 7), consistent with a previous study which showed that MSH6 phosphorylation does not mediate its interaction with MSH2 [20]. Importantly, the MSH6-MSH2 interaction was impaired in MOCS2-knockdown cells, although we did not observe a significant interaction of MOCS2B with MSH6 (Fig. 1A, lanes 6 and 8). We did not observe immunoprecipitated MSH6 in AP-treated MOCS2-knockdown nuclear extracts (Fig. 1A, lane 8), suggesting that dephosphorylation and loss of MOCS2 may impact the stability or conformation of MSH6 [18]. MOCS2 knockdown causes at least two effects: 1) creation of alkylation damage by generating ROS [7], and 2) destabilize MSH6 in an alkylating environment.

We sought to identify proteins which might link MPTAC functions to the roles of MutSα in the nucleus. MPT synthase directly associates with the ATAC complex by binding mitogen-activated protein kinase upstream kinase-binding inhibitory protein (MBIP), an ATAC subunit [5]. Therefore, we examined the interactions of MBIP with MSH6. Indeed, MBIP associated with MSH6 in the nucleus in a MOCS2- and dephosphorylation-dependent manner (Fig. 1A, lanes 7 and 8). To examine whether these interactions were mediated by DNA, we treated the extracts with Benzonase. The associations of MSH2, MBIP, and NC2β (an ATAC subunit) with MSH6 were weaker with Benzonase treatment than without treatment. However, the interactions were intact in Benzonase treated control knockdown cells and required MBIP (Fig. S1A). Purified recombinant MBIP directly interacted with recombinant MSH6 (Fig. 1B), although the interaction of MBIP with MSH 6 was MOCS2-dependent in extracts (Fig. 1A, lanes 7 and 8). We did not observe significant immunoprecipitated MSH6 in MBIP-knockdown extracts treated with AP (Fig. 1C, lane 6, Fig. S1A), suggesting that MBIP also affects the stability of dephosphorylated MSH6. To examine whether these interactions were associated with guanine, we probed the interaction with G protein alpha inhibiting activity polypeptide 2 (GNAI2A), since each α, β, and γ subunit of G-proteins contains a single guanine nucleotide-binding site [21]. GNAI2A expression levels were reduced in MBIP-knockdown cells (Fig. 1C, lane 3, and Fig. S1A). This influenced the association of GNAI2A with MSH6 in a MOCS2- and MBIP-knockdown cells (Fig. 1C, lanes 4–6, Fig. S1A). Together, MOCS2 and MBIP are required for the formation of MutSα and its interaction with GNAI2 and MBIP.

To further examine whether the association of ATAC with MSH6 led to mismatch repair, we examined the interaction of MSH6 with MutLα (a heterodimer of PMS2 and MLH1 [14]) and ATAC in nuclear extracts treated with AP. MutLα expression was reduced (Fig. 1C, lanes 2 and 3) and the interactions of MSH2 and MLH1 with MSH6 were reduced in MOCS2- and MBIP-knockdown cells (Fig. 1C, lanes 5 and 6). Thus, O^6meG:T promotes MutLα recruitment for MMR in a MOCS2- and MBIP-dependent manner. Stabilization of dephosphorylated MSH6 by MOCS2 and MBIP is crucial for recognition of O^6meG-T and for MutLα recruitment. Remarkably, the interactions of MSH6 with ATAC subunits, ADA2A, ZZZ3, and MBIP were reduced in MOCS2- and MBIP-knockdown cells [22,23] (Fig. 1C). Therefore, we examined the effects of MOCS2 and MBIP in the formation of ATAC by ADA2A immunoprecipitation. We found that the interactions of NC2β and MBIP with ADA2A were abolished although the interaction of ZZZ3 with ADA2A was maintained in MOCS2- and MBIP-knockdown cells (Fig. 1D), indicating that ATAC is partially disrupted in MOCS2- and MBIP-knockdown cells. Together, MOCS2 and ATAC are crucial for MMR in response to alkylation damage.

Ubiquitin-specific peptidase 9, Y-linked (USP9Y) has been shown to co-immunoprecipitate with MutL homologue PMS1, which forms heterodimers with MLH1 [24]. USP9 and USP7 are recruited by ovarian tumor family deubiquitinase 4 (OTUD4) to promote repair of alkylated DNA lesions via stabilization of ALKBH2/3[25]. *USP9Y* is 91% identical with *USP9X* [26]. Therefore, we examined the interactions between USP9X, MPTAC, and ATAC in the promotion of MMR using female HEK293 cells. In the nucleus, protein levels of MSH2, MSH6, and USP9X

A

Knockdown	MOCS2
Genes regulating lipid metabolism	*HMGCS1* *NSDHL* *NAPEPLD*
Others	*HIF1A* *GNAI3* *HIGD1A* *TMSB4X* *GTPBP8*

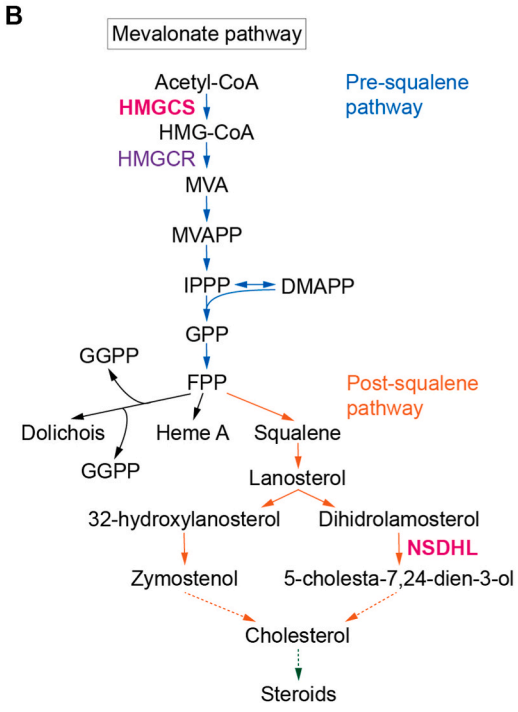

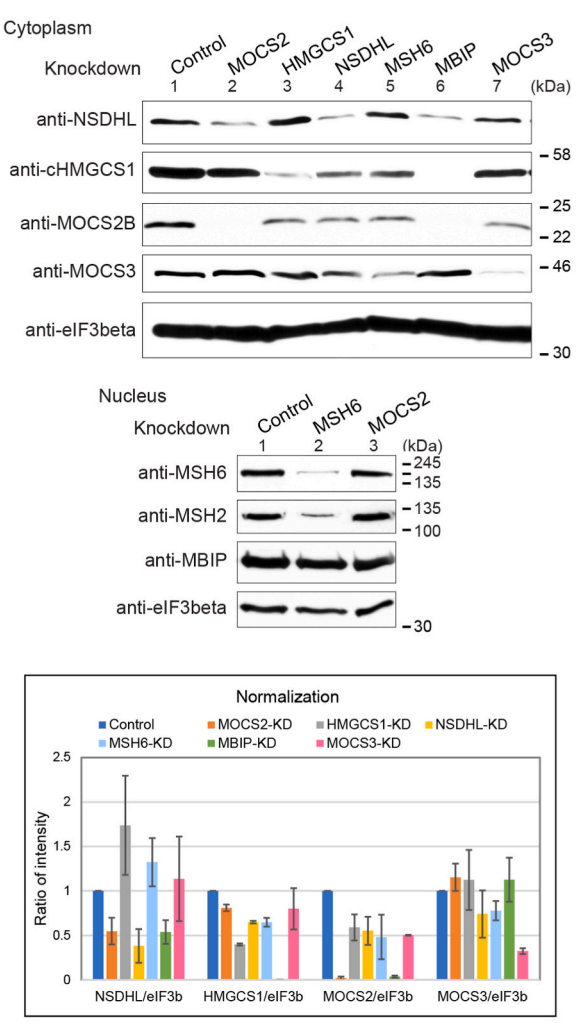

Fig. 2. MPTAC translationally regulates the sterol biosynthesis.
(A) Genes involved in cholesterol synthesis were significantly (RPKM>1) downregulated in polysome fractions from MOCS2-knockdown cells. NAPEPLD, N-acyl phosphatidylethanolamine phospholipase D; GNAI3, G protein subunit alpha i3; HIGD1A, HIG1 hypoxia-inducible domain family member 1A; GTPBP8, GTP binding protein 8 (putative). **(B)** Diagram of the mevalonate pathway in humans. (Abbreviations are defined in the Supplementary materials). **(C)** Cytoplasmic and nuclear extracts from indicated knockdown HEK293 cells were analyzed by Western blot. eIF3β was used as the loading control. The band intensities (signals) for NSDHL, cytoplasmic HMGCS1, MOCS2B, and MOCS3 in cytoplasm were quantified and plotted as averaged ratios ± SD of each signal relative to each eIF3β signal (n = 2) (upper right panel).

were reduced in MBIP-knockdown cells treated with AP for an hour (Fig. S1B, lane 5). The interactions of USP9X with MSH6 and ATAC were reduced in MOCS2- and MBIP-knockdown cells (Fig. 1C and D). Cytoplasmic expression of MOCS3, a subunit of MPTAC, was reduced in USP9X-knockdown cells, although MOCS2 expression was unchanged in USP9X-knockdown cells (Fig. S1C). We also tested control extracts treated with temozolomide (TMZ), a DNA alkylating agent that targets O^6G [27], to investigate whether the interactions of USP9X respond to an alkylating environment. USP9X was clearly associated with MOCS3 in the cytoplasm in a MOCS2- and MBIP-dependent manner, and this association was retained upon TMZ treatment (Fig. 1E, lanes 4–6; S1D, lanes 5–8). However, the interactions of MOCS3 with MSH6, HSD17B10 (a MPTAC subunit [7]), and MOCS2 were weaker in the control treated with TMZ (Fig. 1E). MOCS2 is required for the formation of MPTAC [7], and MBIP knockdown reduces MOCS2 expression (Fig. S1C). Therefore, these data suggested that formation of MPTAC is important for the association of MOCS3 with USP9X. A strong alkylating environment may promote MSH6 degradation and MPTAC disruption in the cytoplasm. Importantly, the association of MLH1, PMS1, and MSH6 with USP9X in the nucleus requires MOCS2 and MBIP (Fig. 1C, lanes 4–6; S1E, lanes 5–7). Together, MMR proteins are stabilized by their interactions with MPTAC and ATAC, which are mediated by association between USP9X, MOCS3, MOCS2, and MBIP (Fig. 1F). ATAC is especially crucial for MutSα formation.

3.2. *MPTAC regulates the mevalonate pathway*

We next investigated whether DNA mismatch repair is related to features of MPTAC. We previously found that MOCS2-dependent metabolism is required for mRNA processing and translation [7,16]. We found that XDH is required for MOCS2 mRNA loading onto polysomes, and MOCS2 is required for HIF1A mRNA loading, by RNA-sequencing of polysome fractions in MOCS2- and XDH-knockdown cells [16] (Fig. 2A). In this study, we found that transcripts of 3-hydroxyl-3-methylglutaryl-CoA synthase 1 (*HMGCS1*), which initiates the mevalonate pathway and sterol byosyntheis [28], were significantly reduced in polysomes of MOCS2-knockdown cells (Fig. 2A). In the ketone synthesis reaction, excess acetyl-CoA is converted to

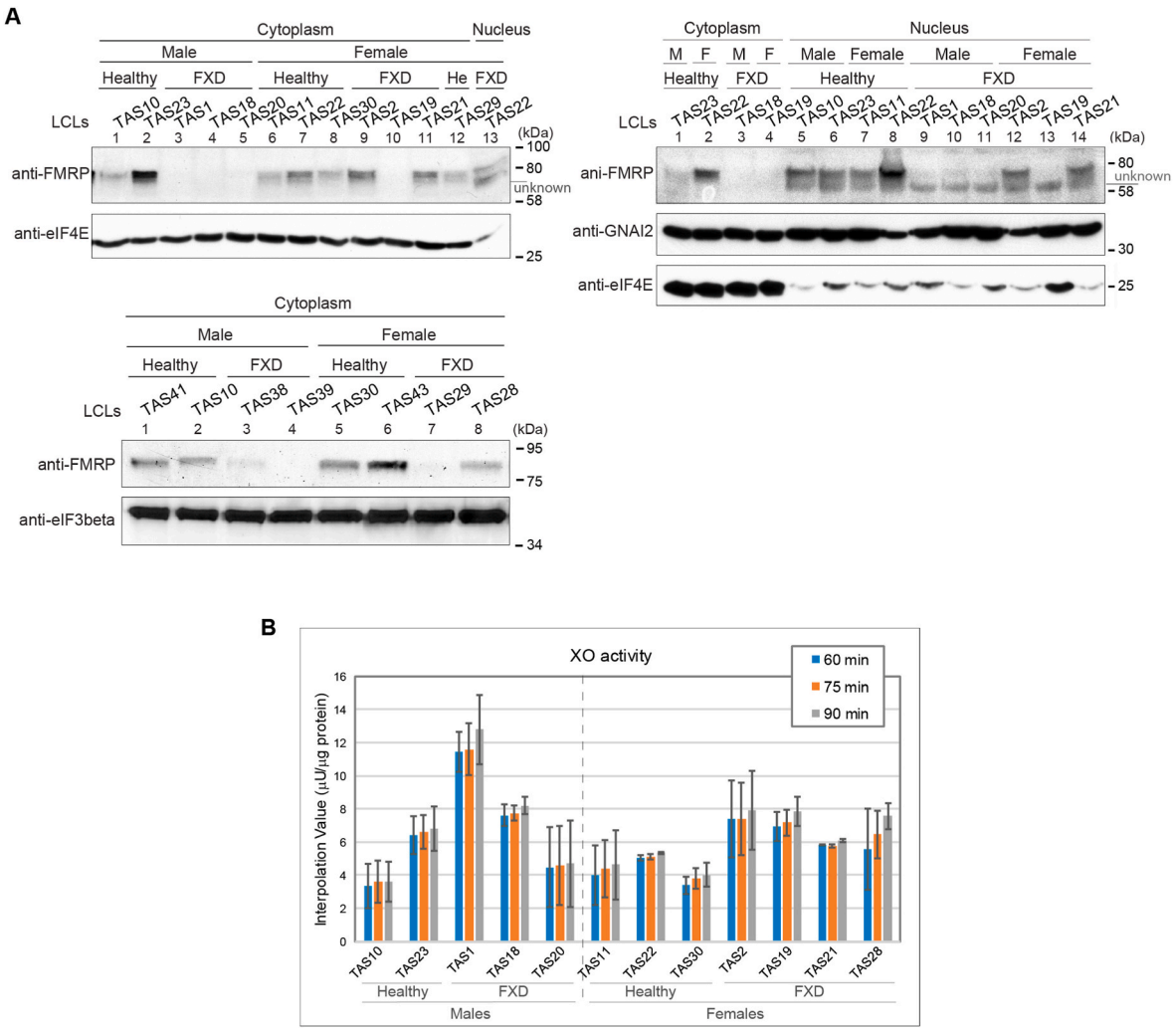

Fig. 3. Xanthine oxidase activity is elevated in LCLs from FXD patients.
(A) FMRP levels in LCLs were examined by Western blot. eIF4E/eIF3β was the loading control (Table S1). **(B)** Xanthine oxidase (XO) activity in cytoplasmic extracts of LCLs were measured by fluorometric assay (mean ± SD, n = 2).

hydroxymethylglutaryl CoA (HMG-CoA), a precursor of cholesterol and an intermediate of the primary ketone body in the blood [28] (Fig. 2A and B). Transcripts of NAD(P)-dependent steroid dehydrogenase-like (*NSDHL*) were dependent on MOCS2 (Fig. 2A and B). Furthermore, transcript levels of thymosin beta 4 X-linked (*TMSB4X*), which reduces production of proinflammatory cytokines [29] were significantly reduced in MOCS2-knockdown cells (Fig. 2A). Thus, MOCS2 crucially regulates translation of genes responding to inflammation.

Importantly, protein levels of HMGCS1, MOCS2, and MOCS3 were reduced but NSDHL levels were increased in MSH6-knockdown cells versus control cells (Fig. 2C, lane 5, S2). NSDHL expression was heterogeneous, including large depositions in MSH6-knockdown cells compared to controls (Fig. S2). Thus, MMR tolerance by MSH6-knockdown attenuates the pre-squalene pathway and promotes sterol synthesis, as seen in HMGCS1-knockdown cells (Figs. 2C and S2). Importantly, MBIP is critical for MSH6 expression and the mevalonate pathway, and associates with MSH6 and MOCS2 (Fig. 1B–D, 2C). Therefore, ATAC is essential for the connections of MPTAC and MMR to the mevalonate pathway and sterol synthesis through the association of ATAC with MPTAC and MSH6.

3.3. *Xanthine oxidase activity is elevated in lymphoblastoid cell lines from FXD patients*

We asked whether these feature of MPTAC and ATAC are related to clinical disorders. A previous study showed that total cholesterol and low and high density lipoprotein were significantly reduced in male FXS cohorts relative to age-adjusted population normative data. Females carrying *FMR1* premutation alleles have a 46.4% greater risk of immune-mediated disease than female noncarriers [30]. Steroids are generated from cholesterol and also reduce the activity of immune system [31]. Increased Aβ deposition, which is suppressed by MPTAC [7], was found to be increased in *Fmr1*-knockout mice [9]. Therefore, we examined the involvement of MPTAC in FXD. We first analyzed the protein levels of FMR1 protein (FMRP) in LCLs from: 1) five male FXS patients who carry large CGG expansions and have neurological disorders (TAS1/18/20/38/39); 2) two females whose FXS diagnosis is unknown but who have family members diagnosed with FXS (TAS2/29) (TAS29 carries a premutation allele); 3) two females diagnosed with FXS (TAS19/21); and 4) a female with a negative diagnosis for FXS but whose family members are diagnosed with FXS (TAS28) (Table S1). FMRP was not expressed in LCLs from any of the male FXS patients (TAS1/18/20/38/39) or in LCLs from one of the two female FXS patients (TAS19) and one female carrying a permutation alle (TAS29) (Fig. 3A). FMRP was expressed in LCLs from the other female FXS patient (TAS21)

Suganuma Fig. 4

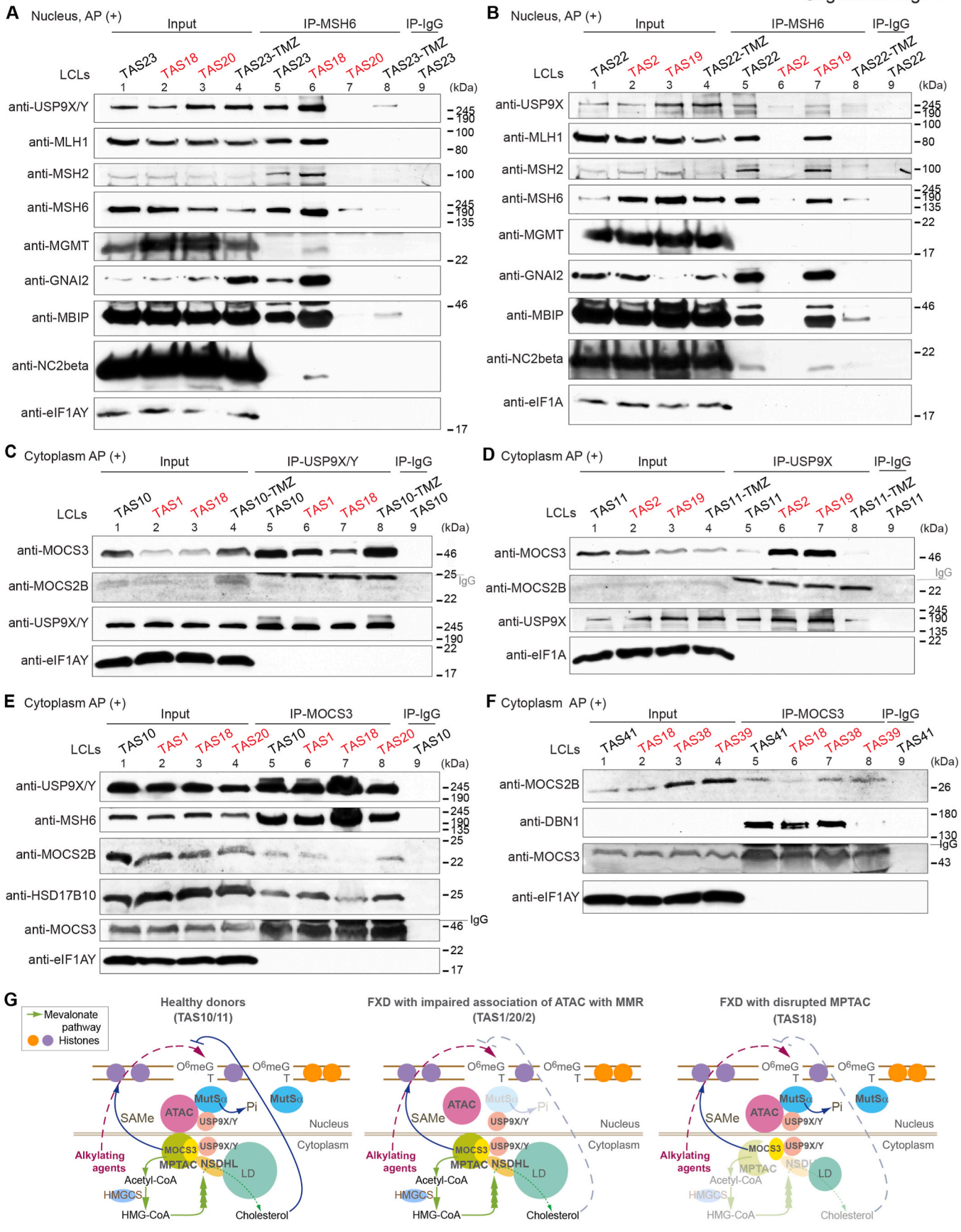

(caption on next page)

Fig. 4. Interactions of MMR proteins with ATAC or MPTAC are disrupted in LCLs from FXD.
(A and B) MSH6 immunoprecipitation (IP) in nuclear extracts from LCLs of male (A) and female (B) FXD patients (red) and from LCLs from healthy donors (TAS22/23) treated with 100 mM TMZ for 48 h were examined by Western blot. IgG immunoprecipitants were used as a control. HGMT, O^6-methylguanine DNA methyltransferase. eIF1AY/eIF1A was used as the loading control. **(C and D)** USP9X/Y IP in AP-treated cytoplasmic extracts from LCLs from male (C) and female (D) FXD patients (red) were examined by Western blot. LCLs from healthy donors (TAS10/11) treated with 100 mM TMZ for 48 h were also examined. IgG immunoprecipitants were used as a control. **(E and F)** MOCS3 IP in AP-treated cytoplasmic extracts from male LCLs were examined by Western blot. **(G)** Model summarizing how DNA mismatch repair (healthy) is reprogrammed by disruption of MPTAC (TAS18) or dissociation of ATAC from MutSα (TAS20/2) as observed in LCLs from FXD patients. . (For interpretation of the references to colour in this figure legend, the reader is referred to the Web version of this article.)

and from the two females with familial FXS but unknown FXS diagnosis (TAS2) (Fig. 3A). Here after, we refer these patients' cells as FXD cells.

We next examined inflammatory responses in the FXD cells. Inflammatory cytokines induce XDH expression [2]; thus, we measured xanthine oxidase activity in LCLs, as XDH is rapidly converted to XO in the inflammatory environment [2]. XO activity in LCLs from female FXD patients was significantly higher than in LCLs from healthy female donors (Fig. 3B). XO activity in male FXD patients was also higher than in healthy male donors, though there was greater variation in XO activity in the males than in the females (Fig. 3B). Therefore, compared to healthy donors, increased XO activity is not observed in only patients with FXS diagnosis but also in patients with FXS family members.

3.4. Impaired MPTAC leads to alkylation damage resistance in LCLs from FXD patients

Since increased XO activity causes ROS production [3,32], we investigated whether functions of MPTAC in MMR are involved in alkylating environment of FXD. We also examined the extracts of LCLs from healthy donors treated with TMZ, the DNA alkylating agent specific to O^6G, as a control [27]. The associations of MLH1, MSH2, and MBIP with MSH6 were diminished in cells from some FXD patients (TAS20/2/1) and in TMZ-treated healthy donor cells (TAS23-TMZ/-TAS22-TMZ) versus in untreated healthy donor cells (TAS10/23/22) (Fig. 4A, lanes 5, 7, 8; 4B, lanes 5, 6, 8; Fig. S3A). Therefore, the association of MSH6 with MBIP is disrupted by a strong alkylating environment in LCLs. This may lead to alkylating agent resistance in cells from some FXD patients (TAS20/2/1). Conversely, the associations of MSH6 with MBIP and the O^6-methylguanine DNA methyltransferase (MGMT) that directly repairs O^6meG and O6Cl-ethylG lesions by removing the alkyl group from O^6G [14] were greater in cells from a male FXD patient (TAS18) (Fig. 4A, lanes 5 and 6; Fig. S3A). Hence, direct repair and mismatch repair were facilitated in LCLs from TAS18.

In LCLs, association of MOCS2 with USP9 was marginal; however, MOCS3 was clearly associated with USP9 in the cytoplasm (Fig. 4C, lanes 5–8; 4D, lanes 5–7). Associations of USP9X/Y and MSH6 with MOCS3 by MOCS3-immunoprecipitation were also elevated in the cytosol of LCLs from TAS18 (Fig. 4E, lanes 5 and 7). USP9X/Y associated with MSH6 in the nucleus in TAS1/18 LCLs but not in TAS20 LCLs (Fig. 4A, lanes 6 and 7; Fig. S3A). However, the association of MOCS2 with MOCS3 observed in cells from TAS10/1/20 was reduced in TAS18 LCLs (Fig. 4E, lanes 5–8; 4F, lane 6). The association of HSD17B10 (a subunit of MPTAC) with MOCS3 was also reduced in TAS18 LCLs, although MOCS3 maintained associations with MSH6 and USP9X/Y (Fig. 4E, lane 7). Remarkably, the levels of NSDHL and lipid droplets were poor in TAS18 compared to TAS10 cells (Fig. S3B). Thus, MPTAC is disrupted, leading to disruption of mevalonate pathway in TAS18. Notably, the associations of MSH2, MLH1, MBIP, and USP9X with MSH6 were increased, indicating that mismatch repair is facilitated in TAS18 (Fig. 4A, lane 6; Fig. S3A). A previous study showed that resistance to alkylation damage depends on overexpression of alkylation repair proteins [25]. Therefore, these data suggest that disruption of MPTAC may impede feedback to alkylation damage, leading to promotion of MMR (Fig. 4G). The disruption of MPTAC may have led to resistance to alkylation damage in TAS18.

In females, association of MOCS3 with USP9X in the cytoplasm was greater in FXD cells (TAS2/19) than in cells from a healthy donor (TAS11), based on USP9X immunoprecipitation (Fig. 4D, lanes 5–7). However, the association of USP9X with MSH6 in the nucleus was reduced in TAS2 (Fig. 4B, lanes 5 and 6), indicating that USP9X is predominantly associated with MOCS3 in TAS2/19 and is dissociated with MSH6 in TAS2. Importantly, the association of MBIP with MMR proteins is impaired in TAS2 (Fig. 4B, lane 6). We further asked whether disruption of the MPTAC was observed in LCLs from other FXD patients (Table S1). We found that the association of the MPTAC subunit drebrin 1 (DBN1) with MOCS3 was greatly reduced in cells of the male FXD patient TAS39 (Fig. 4F). These data suggested that mismatch repair may perturbed due to disruption of MPTAC in TAS39.

4. Conclusion

Alkylating agents promote DNA mismatch repair, which facilitates the mevalonate pathway through interaction of MPTAC with ATAC, leading to an anti-inflammatory response, and reducing alkylation damage. Therefore, MPTAC may moderate alkylation damage and stabilize MSH6, regulating MutSα expression (Fig. 4G Healthy). ATAC associates with and stabilizes MSH6 upon alkylation damage. However, in LCLs of some FXD patients, disruption of MPTAC (TAS18/39) or impaired association of ATAC with MSH6 (TAS1/20/2) fail to moderate alkylation damage (Fig. 4G FXD). Some FXD patients may have obtained resistance to alkylating agents. Disruptions of MPTAC or ATAC-MMR dissociation were not only observed in LCLs with loss of FMRP (a bona fide FXS) (TAS1/18/20/39) but also LCLs from FXD patients expressing FMRP (TAS2). Further statistical studies will advance our understanding of the involvement of alkylating agents on *Fmr1* mutations and clinical symptoms.

Funding

This research was supported by the Stowers Institute for Medical Research and NIH grant R35GM118068.

Declaration of competing interest

The authors declare no conflicts of interests.

Acknowledgements

We thank Dr. Juliana Conkright-Fincham and Ms. Carolyn Beucher for technical support.

Appendix A. Supplementary data

Supplementary data to this article can be found online at https://doi.org/10.1016/j.redox.2022.102270.

References

[1] N. Vassilaki, E. Frakolaki, Virus-host interactions under hypoxia, Microb. Infect. 19 (2017) 193–203.
[2] N. Cantu-Medellin, E.E. Kelley, Xanthine oxidoreductase-catalyzed reactive species generation: a process in critical need of reevaluation, Redox Biol. 1 (2013) 353–358.
[3] G. Schwarz, R.R. Mendel, M.W. Ribbe, Molybdenum cofactors, enzymes and pathways, Nature 460 (2009) 839–847.

[4] K.B. Schwarz, Oxidative stress during viral infection: a review, Free Radical Biol. Med. 21 (1996) 641–649.
[5] T. Suganuma, S.K. Swanson, L. Florens, M.P. Washburn, J.L. Workman, Moco biosynthesis and the ATAC acetyltransferase engage translation initiation by inhibiting latent PKR activity, J. Mol. Cell Biol. 8 (2016) 44–50.
[6] A.I. Papadakis, et al., eIF2{alpha} Kinase PKR modulates the hypoxic response by Stat3-dependent transcriptional suppression of HIF-1{alpha, Cancer Res. 70 (2010) 7820–7829.
[7] T. Suganuma, et al., MPTAC determines APP fragmentation via sensing sulfur amino acid catabolism, Cell Rep. 24 (2018) 1585–1596.
[8] A. Matthies, K.V. Rajagopalan, R.R. Mendel, S. Leimkuhler, Evidence for the physiological role of a rhodanese-like protein for the biosynthesis of the molybdenum cofactor in humans, Proc. Natl. Acad. Sci. U. S. A. 101 (2004) 5946–5951.
[9] C.J. Westmark, et al., Reversal of fragile X phenotypes by manipulation of AbetaPP/Abeta levels in Fmr1KO mice, PLoS One 6 (2011), e26549.
[10] D.C. Crawford, J.M. Acuna, S.L. Sherman, FMR1 and the fragile X syndrome: human genome epidemiology review, Genet. Med. : official journal of the American College of Medical Genetics 3 (2001) 359–371.
[11] P.J. Hagerman, R.J. Hagerman, Fragile X-associated tremor/ataxia syndrome, Ann. N. Y. Acad. Sci. 1338 (2015) 58–70.
[12] T.I. Winarni, et al., Immune-mediated disorders among women carriers of fragile X premutation alleles, Am. J. Med. Genet. 158A (2012) 2473–2481.
[13] Y. Liu, T.I. Winarni, L. Zhang, F. Tassone, R.J. Hagerman, Fragile X-associated tremor/ataxia syndrome (FXTAS) in grey zone carriers, Clin. Genet. 84 (2013) 74–77.
[14] D. Fu, J.A. Calvo, L.D. Samson, Balancing repair and tolerance of DNA damage caused by alkylating agents, Nat. Rev. Cancer 12 (2012) 104–120.
[15] J.M. Soll, R.W. Sobol, N. Mosammaparast, Regulation of DNA alkylation damage repair: lessons and therapeutic opportunities, Trends Biochem. Sci. 42 (2017) 206–218.
[16] T. Suganuma, et al., MOCS2 links nucleotide metabolism to nucleoli function, J. Mol. Cell Biol. 13 (2022) 838–840.
[17] S. Kaliyaperumal, S.M. Patrick, K.J. Williams, Phosphorylated hMSH6: DNA mismatch versus DNA damage recognition, Mutat. Res. 706 (2011) 36–45.
[18] M.A. Edelbrock, S. Kaliyaperumal, K.J. Williams, Structural, molecular and cellular functions of MSH2 and MSH6 during DNA mismatch repair, damage signaling and other noncanonical activities, Mutat. Res. 743–744 (2013) 53–66.
[19] N. Papadopoulos, et al., Mutations of GTBP in genetically unstable cells, Science 268 (1995) 1915–1917.
[20] M. Christmann, M.T. Tomicic, B. Kaina, Phosphorylation of mismatch repair proteins MSH2 and MSH6 affecting MutSalpha mismatch-binding activity, Nucleic Acids Res. 30 (2002) 1959–1966.
[21] T. Asano, R. Morishita, K. Kato, Identification of a guanine nucleotide-binding protein G(o) in human neuroblastoma, Cancer Res. 48 (1988) 2756–2759.
[22] T. Suganuma, et al., ATAC is a double histone acetyltransferase complex that stimulates nucleosome sliding, Nat. Struct. Mol. Biol. 16515 (2008) 364–372.
[23] T. Suganuma, et al., The ATAC acetyltransferase complex coordinates MAP kinases to regulate JNK target genes, Cell 142 (2010) 726–736.
[24] E. Cannavo, B. Gerrits, G. Marra, R. Schlapbach, J. Jiricny, Characterization of the interactome of the human MutL homologues MLH1, PMS1, and PMS2, J. Biol. Chem. 282 (2007) 2976–2986.
[25] Y. Zhao, et al., Noncanonical regulation of alkylation damage resistance by the OTUD4 deubiquitinase, EMBO J. 34 (2015) 1687–1703.
[26] S. Colaco, D. Modi, Genetics of the human Y chromosome and its association with male infertility, Reprod. Biol. Endocrinol. : RBE (Rev. Bras. Entomol.) 16 (2018) 14.
[27] C.R. Gil Del Alcazar, P.K. Todorova, A.A. Habib, B. Mukherjee, S. Burma, Augmented HR repair mediates acquired temozolomide resistance in glioblastoma, Mol. Cancer Res. : MCR 14 (2016) 928–940.
[28] M. Moutinho, M.J. Nunes, E. Rodrigues, The mevalonate pathway in neurons: it's not just about cholesterol, Exp. Cell Res. 360 (2017) 55–60.
[29] H.K. Kleinman, G. Sosne, Thymosin beta 4 promotes dermal healing, Vitam. Horm. 102 (2016) 251–275.
[30] A.C. Wheeler, et al., Associated features in females with an FMR1 premutation, J. Neurodev. Disord. 6 (2014) 30.
[31] Y. Yamauchi, M.A. Rogers, Sterol metabolism and transport in atherosclerosis and cancer, Front. Endocrinol. 9 (2018) 509.
[32] N. Vassilaki, et al., Low oxygen tension enhances hepatitis C virus replication, J. Virol. 87 (2013) 2935–2948.